Model-based evaluation of reduction strategies for point and nonpoint source Cd pollution in a large river system

Lingfeng Zhou[a], Xiaoli Zhao[a], Miaomiao Teng[a], Fengchang Wu[a*], Yaobin Meng[b], Yating Wu[b], Patrick Byrne[c], Karim C. Abbaspour[d]

[a]State Key Laboratory of Environmental Criteria and Risk Assessment, Chinese Research Academy of Environmental Sciences, Beijing, 100012, China

[b]School of National Safety and Emergency Management, Beijing Normal University, Beijing, 100875, China

[c]School of Biological and Environmental Sciences, Liverpool John Moores University, Liverpool, L3 3AF, UK

[d]2w2e Consulting, GmbH, Mettlenweg 3, 8600 Duebendorf, Switzerland

*Corresponding author: Dr. Fengchang Wu

E-mail: wufengchang@vip.skleg.cn

Abstract

Cadmium (Cd) is a toxic trace element that threatens ecosystem and human health worldwide. Quantitative understanding of land-to-river Cd fluxes and riverine Cd loads in response to various watershed management measures is essential for developing effective mitigation strategies for large river systems. However, detailed analyses of watershed Cd dynamics under different management scenarios are lacking. Here, we investigated the effects of four management scenarios by combining point and nonpoint source control measures with a previously developed watershed Cd model that was validated with site-specific measurements. The Soil and Water Assessment Tool-Heavy Metal (SWAT-HM) model was applied to simulate the Xiang River Basin's (XRB, ~90,000 km^2) baseline hydrology, soil erosion, and Cd transport processes in China. Using scenario simulations, we found that smelting emissions reduction was the most influential measure for controlling dissolved Cd (DCd) and particulate Cd (PCd) loads at the basin scale. Elimination of 50% emissions from the smelting sector could significantly ($p < 0.05$) decrease the monthly mean loads of DCd from 940 to 720 kg and of PCd from 2,150 to 1,760 kg at the XRB outlet. In contrast, reduction in mining emissions had no influence on the Cd load at the XRB outlet because most mining Cd emissions occurred upstream and midstream of the XRB, and the natural attenuation processes in the river limit the transportation of Cd downstream. The effectiveness of management practices for reducing total Cd (TCd) and DCd loads was not always mutually beneficial. For example, soil erosion control may decrease the PCd flux *via* erosion but increase the subsurface DCd flux to rivers due to greater lateral flow. In addition, increasing soil pH could be a practical and effective measure to reduce nonpoint DCd and PCd fluxes. Such effects may be caused by the declined upward migration of Cd through soil evaporation owing to the decreased Cd concentration in the soil pore water after pH

increases. In conclusion, effective watershed management of Cd pollution in large basins requires an integrated plan that combines multiple mitigation measures; strategic modeling experiments could provide valuable insights into the design of such plans.

Keywords: Cadmium loads; Watershed model; Scenario analysis; Nonpoint source pollution; Industrial point emission; Watershed management

1. Introduction

Cadmium (Cd), classified as a group 1 human carcinogen (IARC, 2018), is a global threat to terrestrial and aquatic ecosystems and human health (Kubier et al., 2019; Satarug et al., 2003; Satarug et al., 2017; WHO, 2010). Industrial (e.g., mining and smelting) and agricultural (e.g., phosphate fertilizers) activities have discharged a large amount of Cd into soils and water worldwide, including in Europe and China (Nziguheba and Smolders, 2008; Shi et al., 2019; Ulrich, 2019). Human activities have increased soil Cd concentrations by approximately 0.1–0.3 mg Cd kg^{-1} above pre-industrial levels (Smolders and Mertens, 2013). The long-term dietary intake of Cd at elevated levels can lead to serious health problems, such as the "Itai-itai" disease that occurred in Japan in the 1950s (Aoshima, 2016). A 2014 national soil survey in China showed that Cd is the most serious contaminant, accounting for 43% of all soil quality exceedances (MEPPRC and MLRPRC, 2014). In addition, millions of hectares of agricultural land in China are now being removed from production due to Cd pollution (Hou and Li, 2017). Moreover, soil Cd concentrations continue to increase despite stricter environmental protection regulations (Hu et al., 2016).

According to a meta-analysis of the global evaluation of heavy metal pollution in surface water, China reported the most pollution sites of heavy metals, followed by India and other developing countries (Kumar et al., 2019). China's river basins have experienced extensive metal pollution over the past decades, with the Xiang River Basin (~90,000 km^2) being the most polluted. The issue of Cd pollution in soil, water, sediment, and rice in the XRB has attracted substantial attention (Han et al., 2014; Li et al., 2018; Williams et al., 2009; Zhang et al., 2008). In 2011, the Chinese central government approved the Xiang River Basin Control Plan for Heavy Metal Pollution (hereafter XRB Plan) to combat severe heavy metal pollution (http://www.gov.cn/gzdt/2011-

07/23/content_1912271.htm). This ambitious XRB Plan (declared as the Chinese Rhine project) invested up to 59.5 billion RMB (9.8 billion US Dollars) and focused mainly on the industrial sectors to reach the 50% target of metal emission reduction by 2015 from the 2008 level (Hu et al., 2014). However, river pollution mitigation requires holistic accounting for both point and nonpoint (diffuse) sources. Point emissions, such as Zn–Cd smelters, have been stopped in numerous places; however, residual soil Cd contamination remains (e.g., Y. Zhou et al., 2020). Recent studies in UK mined watersheds have demonstrated that the remediation of point sources of metals could be less efficient because of the greater importance of untreated diffuse sources under extremely low flows (groundwater from underground mine workings, Byrne et al., 2020) and extremely high flows (runoff from surface mine wastes, Jarvis et al., 2019). Elevated soil Cd concentrations have been reported in many mining areas of the XRB (e.g., Lei et al., 2015). Moreover, it has long been acknowledged that soil acidification can contribute to increased Cd mobility and loss in soil (e.g., Kicińska et al., 2022). Therefore, a quantitative understanding of land-to-river Cd fluxes and riverine Cd loads in response to different watershed management measures is vital for developing effective mitigation strategies in large-scale complex river networks, such as the Xiang River system.

Numerical models are valuable tools for developing remediation strategies (Nair et al., 2022; Xie et al., 2015; Zhuang et al., 2016). Several watershed-scale heavy metal models with various levels of complexity have been developed to address these challenges, including TREX (Velleux et al., 2008), INCA-Metals (Whitehead et al., 2009), SWAT-HM (Meng et al., 2018), ECOMAG-HM (Motovilov and Fashchevskaya, 2019), and TOPKAPI-ETH (Sui et al., 2022). Generally, two main categories of processes (contaminant transformation and transport) are considered in the watershed-scale metal fate and transport models. Contaminant transport commonly consists of three processes:

(1) overland hydrological processes, (2) soil erosion and sediment transport, and (3) in-stream processes. According to the temporal scales, the models can be divided into event-driven and continuous models. For example, TREX is mainly an event model that can simulate the fate and transport of metals during a single rainfall event at the watershed scale (Velleux et al., 2008). The ECOMAG-HM does not include a sediment component and is inapplicable to erosion-prone areas (Motovilov and Fashchevskaya, 2019). The TOPKAPI-ETH is a fully distributed model that divides the watershed and sub-basins into hydraulically connected grid cells to depict detailed cell-to-cell transport (Sui et al., 2022). However, owing to the computational burden and high demand for data, the application of TOPKAPI-ETH to large-scale basins such as the XRB is limited. In contrast, models such as INCA-Metals and SWAT-HM are semi-distributed, continuous models with reasonable model structural complexity, which enable them to analyze the long-term effects of hydrological changes and water management practices. In this study, we chose SWAT-HM because the SWAT component is a widely used nonpoint source hydrologic model with an open-source code, making it amenable to coupling with other models and expanding the model representation of different environmental management scenarios.

Watershed models have been widely used for scenario analyses to assess the best management practices for sediment, nitrogen, and phosphorus load mitigation (Hunt et al., 2019; Kast et al., 2021; Shen et al., 2015). Thus far, only a few watershed-scale HM models have been used to evaluate the impacts of mitigation practices (Jiao et al., 2014). For example, Whitehead et al. (2009) examined the effects of mine restoration on downstream metal loads, but were limited to point-source cleanup scenarios. Nonpoint source control measures have rarely been considered in the evaluation of watershed management plans, although many studies have suggested that nonpoint pathways play

an important role in watershed-scale metal transport. For instance, Liu et al. (2019) reported that soil conservation projects have reduced the lateral transport of heavy metals by 56% in the Loess Plateau over the past two decades. Moreover, field experiments have shown that liming can effectively increase soil pH and reduce Cd mobility and bioavailability in agricultural lands (Holland et al., 2018).

To the best of our knowledge, a detailed investigation of watershed Cd dynamics under different management scenarios, particularly for large-scale river systems with various point and nonpoint sources, is lacking. Thus, the overall aim of this study was to demonstrate how a watershed-scale HM model can be used to assess the sensitivity of different management scenarios to land-to-river Cd fluxes and riverine Cd loads at various spatiotemporal scales and to develop a feasible and desirable watershed management plan for achieving water quality targets in the XRB. The results of this study support the development of numerical models of Cd fate and transport in large river basins and offer critical insights into the potential impacts of different Cd pollution reduction strategies on water quality.

2. Materials and Methods

2.1. Study area

The Xiang River Basin (E:110°30′–114°15′, N:24°38′–28°39′) is one of the seven major tributaries of the Yangtze River, located in South-Central China, spanning over 9,400 km^2 with a length of 948 km (Fig. 1a). The main stream of the Xiang River flows from south to north and drains into Dongting Lake of the Yangtze River system. The Xiang River can be divided into three main

sections: the upper section from the headstream to Lapbutou, the middle section from Lapbutou to Hengyang, and the lower section from Hengyang to the outlet (Dongting Lake). The major tributaries include the Guan, Chonglin, Zheng, Lei, Mi, Juan, Lu, Lian, Liuyang, Laodao, and Wei Rivers (Fig. 1b). In the XRB, the elevation decreases from south to north, varying from 2,092 m to 7 m. The basin is of a subtropical humid monsoon climate with an annual precipitation of 1,400 mm mainly concentrated between April–September (70%). The main landuses of XRB are forests (FRST, 62.1%), paddy fields (RICE, 20.8%), agricultural land (AGRL, 8.6%), pasture (PAST, 4.0%), and urban areas (1.7%) (Fig. 1c). The river receives massive Cd loads from both point (e.g., industrial emissions) and diffuse sources (e.g., land runoff and erosion). In a previous study (Zhou et al., 2023), we estimated that intensive industrial activities discharged approximately 20,000 kg yr^{-1} of Cd into the Xiang River during 2000–2015. Among them, mining and processing of nonferrous metal ores (hereafter referred to as mining) and smelting and pressing of nonferrous metals (hereafter referred to as smelting) are two main polluters, accounting for 93% of the total industrial Cd emissions. Additionally, many years of historical mining in the XRB have left abandoned mining waste that contributes metal loads to the Xiang River via diffuse processes. Elevated Cd concentrations in soils can also be transported to rivers through hydrological processes and soil erosion. In general, the XRB is representative of many industrialized river basins around the world with point and diffuse sources.

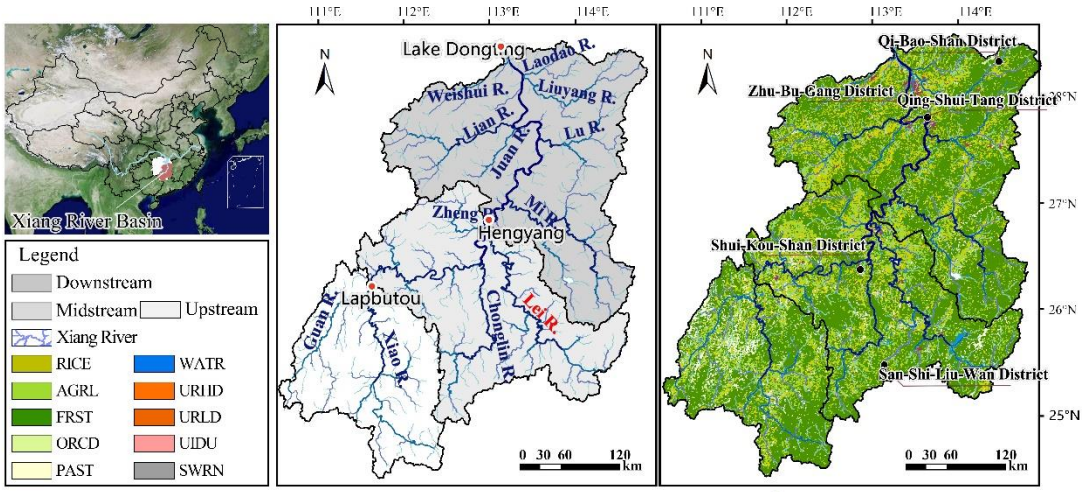

Fig. 1. Study area. (a) Location of the Xiang River Basin in China (b) the river network and up-, mid-, and downstream of XRB (c) land uses in the watershed.

2.2. Watershed-scale Cd model

In our model development paper (Zhou et al., 2023), the SWAT-HM model for the XRB was developed to quantify the flow, sediment, and dissolved Cd (DCd) and particulate Cd (PCd) fluxes in both the land and river phases of the XRB between 2000 and 2015. As discussed in Zhou et al. (2023) and illustrated in Fig. 2, The SWAT-HM, which combines a heavy metal transport and transformation module with the well-established SWAT model (Arnold et al., 1998), is a semi-distributed process-based model for simulating terrestrial metal delivery and riverine metal dynamics. The SWAT model requires Digital Elevation Model (DEM), land use, soil types, and observed meteorological and hydrological and sediment data to run. Point sources (e.g., industrial and municipal metal loads) and nonpoint sources (e.g., soil metal concentrations) data are two main inputs for the HM module. The original version of SWAT-HM was developed by Meng et al. (2018) with a metal transformation module of three-phase (dissolved, labile, and non-labile metal species) equilibrium partitioning and kinetic reactions. However, detailed observations of labile and non-

171 labile metal species in soils are usually not available, especially in large-scale applications such as
172 XRB. The current version was thus modified by simplifying the metal transformation scheme, in
173 which solid labile and non-labile metals are regarded together as particulate metals. This
174 modification maintains a reasonable model structural complexity while considerably minimizing
175 the data requirements. The data requirement of SWAT-HM was summarized in Table 1 of Zhou et
176 al. (2023) with a detailed description in Zhou et al. (2023) SI Text S1. The model was run for extra
177 two years (a warm-up period of 1998–1999) to equilibrate to steady-state conditions. To capture
178 more detailed Cd transport processes and facilitate management scenario analysis, the XRB was
179 divided into 1,118 sub-basins and 23,363 Hydrologic Response Units (HRUs) with the smallest
180 spatial discretization of zero thresholds for land use, soil, and slope in each sub-basin. Prior to this
181 work, parameters have been carefully constrained using multiple field measurements with a 2-
182 step procedure (Zhou et al., 2023). As a first step, SWAT-CUP was used to calibrate and validate
183 parameters related to hydrological and sediment processes (Abbaspour, 2015). To investigate the
184 intrinsic model performance and model defects, five parameters pertaining to metal dynamics were
185 deliberately not calibrated but were instead obtained from field measurements and the literature
186 (Han et al., 2014; Meng et al., 2018; Qin et al., 2012; L. Zhou et al., 2020). The model was validated
187 against long-term historical observations of monthly streamflow and sediment load and Cd
188 concentrations at 42 (4380 data points), 11 (1183 data points), and 10 (600 data points) gauges,
189 respectively. As detailed in Zhou et al. (2023) sections 2.3 and 3.1, the model accuracy was
190 evaluated using both statistical (the coefficient of determination (R^2), Nash-Sutcliffe efficiency
191 (*NSE*), and percent bias (*PBIAS*)) and graphical (scatter plots) analyses. For streamflow, the mean
192 of R^2 and *NSE* were 0.84 and 0.75 with the *PBIAS* ranging from –34.4% to 48.8%. For the sediment

load, the R^2 and *NSE* averaged 0.57 and 0.42, with a *PBIAS* of –61.7% to 39.3%. Approximately 92.0% of the simulated Cd values were within the 5-fold range of the measured concentrations, indicating that the SWAT-HM model was successfully applied to the XRB. The key components of the SWAT-HM are introduced below. For further information on model description and model development in the XRB, see (Meng et al., 2018; L. Zhou et al., 2020; Zhou et al., 2023).

In SWAT, surface runoff (*SR*) was estimated using the SCS curve number method (Eq. 1).

$$SR = \frac{(R-I)^2}{(R-I+S)} \quad (1)$$

where R is the rainfall for the day; I is the initial abstraction, which includes surface storage, interception, and infiltration prior to runoff; and S is the retention parameter, which is a function of the curve number (*CN*) for the day (Eq. 2).

$$S = 25.4\left(\frac{1000}{CN} - 10\right) \quad (2)$$

where *CN* is a function of the soil permeability, land use, and antecedent soil water conditions. CN_2 was defined as the curve number for moisture condition II.

SWAT uses the Modified Universal Soil Loss Equation (MUSLE) to calculate the soil erosion and sediment yield (*SY*) for each HRU within the watershed (Eq. 3).

$$SY = 11.8 \cdot \left(Qq_pA\right)^{0.56} C \cdot P \cdot K \cdot LS \cdot F \quad (3)$$

where Q is the daily runoff volume, q_p is the peak runoff discharge, and A is the HRU area. C, P, and K are the HRU crop cover, soil protection, and soil erodibility factors, as defined in the original Universal Soil Loss Equation (USLE). LS is the USLE topography factor. F is a dimensionless factor that considers the soil stoniness.

In SWAT-HM, soil Cd exists as dissolved Cd ([M_d], mg L^{-1}) in the pore water and particulate Cd (M_p, mg kg^{-1}) in the solid soil, controlled by the partition coefficient (K_d_soil, L kg^{-1}) defined in

Eq. 4, which is a function of the soil pH and soil organic carbon (*SOC*) (Degryse et al., 2009) (Eq. 5).

$$K_d\_\text{soil} = \frac{M_p}{[M_d]} \quad (4)$$

$$K_d\_\text{soil} = 0..55 \cdot pH + 0.70 \cdot \log(SOC) - 1.04 \quad (5)$$

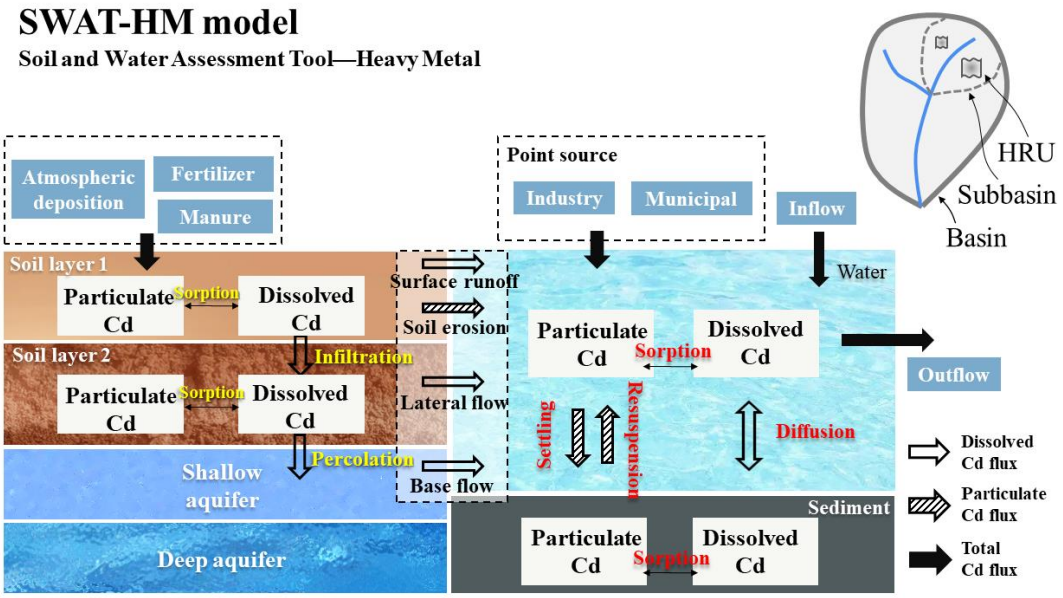

Fig. 2. A schematic diagram of the main processes in both overland and channel phases of the SWAT-HM model.

2.3. Watershed management scenarios planning and analysis

In this study, four management plans that consider both point and nonpoint source pollution control were proposed to mitigate Cd pollution (Table 1). As detailed below, management measures are represented in model simulations by changing the corresponding model inputs or parameter values to depict the changes in watershed processes and water quality responses.

Industrial point source control is the major management measure in the XRB, among which

the mining and smelting sectors are the two main polluters. Scenarios S1.1–S1.5 and S2.1–S2.5 represent the reduction of mining and smelting Cd emissions, respectively, by various percentages (−10%, −20%, −30%, −40%, and −50%). Metal industrial emissions should be reduced by 50%, according to the XRB Plan, which defined targets of 10, 20, 30, 40, and 50%. As an approximation in the model, the same elimination rate is evenly applied to the enterprises in the study area, which is deemed realistic because regulation driven by a regional environmental authority is usually implemented by a uniform requirement for all enterprises. Nonetheless, a uniform elimination rate across different enterprises will have different effects because of the location, and hence, hydrological connectivity disparities.

Scenarios 3.1–3.5 consist of soil erosion control measures. In SWAT, terracing, contour farming, and strip cropping are built-in management operations for soil conservation. For example, the adoption of contour farming permits the reduction of surface runoff by impounding water in small depressions and reduces soil erosion by reducing the erosive power of surface runoff (Arabi et al., 2007). To represent contouring practice, the SCS curve number for moisture condition II (CN_2) and USLE practice factor (*USLE_P*) were modified. In Scenario 3.1–3.5, the improvement in water infiltration was represented by reducing the calibrated CN_2 value by 1, 2, 3, 4, and 5 units. In addition, the *USLE_P* factor, which represents the ratio of soil loss by a support practice to that of straight-row farming up and down the slope, was reduced by 10%, 20%, 30%, 40%, and 50%. The adjustment values for CN_2 and *USLE_P* were within the ranges suggested by Tuppad et al. (2010).

Scenarios 4.1–4.5 correspond to the implementation of soil remediation measures to increase the soil pH. Soil pH is the most prominent factor affecting metal partitioning in acidic soil, to control the mobility and bioavailability of metals (Eq. 5). To control soil pH, lime (CaO or $Ca(OH)_2$), soda

ash (sodium carbonate, Na_2CO_3), sodium hydroxide, and to a lesser extent, magnesium hydroxide are most commonly used; liming to increase soil pH is an effective and economical option (Zhu et al., 2016). Therefore, we derived Scenarios 4.1–4.5 by simply increasing soil pH by 0.1, 0.2, 0.3, 0.4, and 0.5 unit, respectively. The increase in cap (by 0.5) was deemed practically attainable. For example, the application of 7.5 t ha^{-1} $CaCO_3$ could increase soil pH from 5.5 to 6.5 at paddy sites (Chen et al., 2018).

The baseline scenario (S0) represents the reference condition of watershed processes using calibrated parameters and default inputs (Zhou et al., 2023). All scenarios, including the baseline scenario, were simulated using 16-year historical climate records from 2000−2015.

Given the spatial variability of Cd loads, management practices were implemented at priority sites within the watershed. Since the XRB Plan was approved in 2011 and started in 2012, we identified 196 river sections (Fig. 3a) where the monthly TCd concentration in 2012–2015 exceeded the Class Ⅲ (1.0 μg L^{-1}) of the Environmental Quality Standard for Surface Water (GB 3838-2002). Furthermore, 344 upstream sub-basins (Fig. 3b) of these polluted river sections were selected as priority management areas. Finally, 6,955 HRUs (Fig. 3c) with 6 specific land uses (forests (FRST), paddy fields (RICE), agricultural land (AGRL), orchard (ORCD), pasture (PAST), and barren land (SWRN)) were selected as management areas for nonpoint source control (i.e., soil erosion control (S3.1–3.5) and soil pH elevation (S4.1–4.5)).

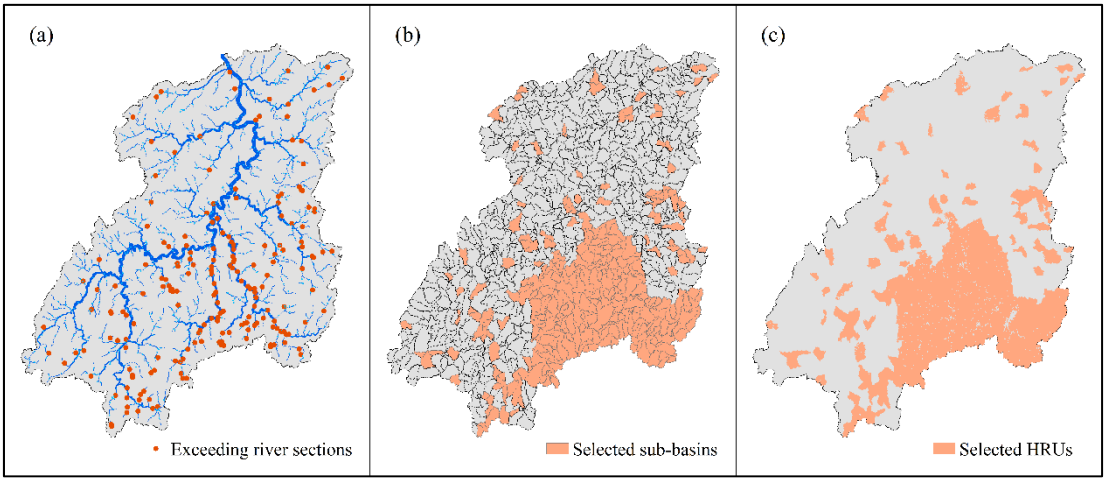

Fig. 3. (a) The river sections exceeding the water quality standard (1.0 μg L^{-1}, GB 3838-2002) during 2012–2015, (b) selected sub-basins, and (c) HRUs for implementing point and nonpoint source control measures in XRB.

Table 1. Management scenarios run through the XRB SWAT-HM model

	Scenario code	Specific settings: modified parameters and inputs in scenario simulations	Management description
Baseline	S0	Default	None
Industrial emissions for mining sector[1]	S1.1	Mining * (1 − 10%)	The impact of different emission reduction levels of the mining sector on downstream Cd load is related to the industrial emission intensity and spatial layout.
	S1.2	Mining * (1 − 20%)	
	S1.3	Mining * (1 − 30%)	
	S1.4	Mining * (1 − 40%)	
	S1.5	Mining * (1 − 50%)	
Industrial emissions for smelting sector[1]	S2.1	Smelting * (1 − 10%)	The impact of different emission reduction levels of the smelting sector on downstream Cd load is related to the industrial emission intensity and spatial layout.
	S2.2	Smelting * (1 − 20%)	
	S2.3	Smelting * (1 − 30%)	
	S2.4	Smelting * (1 − 40%)	
	S2.5	Smelting * (1 − 50%)	
Soil erosion control	S3.1	*USLE_P* * (1 − 10%); CN_2 − 1	Implementing soil conservation measures by changing the parameter values of CN_2 and USLE_P (Arabi et al., 2007)
	S3.2	*USLE_P* * (1 − 20%); CN_2 − 2	
	S3.3	*USLE_P* * (1 − 30%); CN_2 − 3	
	S3.4	*USLE_P* * (1 − 40%); CN_2 − 4	
	S3.5	*USLE_P* * (1 − 50%); CN_2 − 5	
Soil remediation (soil pH control)	S4.1	pH + 0.1	Liming to increase soil pH of top and second soil layers (Chen et al., 2018)
	S4.2	pH + 0.2	
	S4.3	pH + 0.3	
	S4.4	pH + 0.4	
	S4.5	pH + 0.5	

[1]Mining is short for Mining and Processing of Nonferrous Metal Ores, Smelting is short for Smelting and Pressing of Nonferrous Metals.

3. Results and Discussion

3.1. River sections exceeding the water quality standards

First, we investigated the spatiotemporal patterns of Cd concentrations in the Xiang River system based on the baseline model validated with site-specific measurement. Fig. 4a displays the river sections where the monthly mean concentrations of TCd exceeded the water quality standard (GB3838-2002) of 1.0 μg L^{-1} for the up-, mid-, and downstream regions. In general, the exceedance frequency increased first and then declined from 2000 to 2015. The midstream has the highest exceeding rates, ranging from 5.4% to 15.9%, with upstream and downstream having a range of 0.6–7.9% and 1.2–10.7%, respectively. In Fig. 4b, a spatial analysis revealed that most river sections with high exceeding frequency (> 75%) were clustered in the southeast of the XRB (part of the midstream region in Fig. 1) because of the high mining emissions and low dilution capacity. Furthermore, we compared the point Cd fluxes (industrial emissions) and nonpoint Cd fluxes (surface runoff + lateral flow + soil erosion) between the non-exceeding and exceeding river sections. The comparison was made at both the sub-basin and upstream basin level, since riverine Cd loads originate from both upstream channels and sub-basins. At the sub-basin level, the exceeding river sections (red dots in Fig. 4c) occurred under large ranges of point and nonpoint Cd fluxes, which showed no obvious difference from the non-exceeding river sections (blue dots in Fig. 4c). In contrast, the accumulative point and nonpoint Cd fluxes of the upstream sub-basins were also compared. At the upstream basin level, the exceeding river sections (red dots in Fig. 4d) were generally clustered in the region of large point/nonpoint ratios, indicating the dominant role of industrial emissions on riverine Cd load (Fig. 4d). For example, sub-basin outlet 164 (Fig. 4b) is

298 located at the downstream of Qing-Shui-Tang industrial district, which is the largest industrial
299 district in XRB and contributes 21.7% of the total industrial Cd emissions between 2000 and 2015
300 (Zhou et al., 2023). However, there also exist some exceeding river sections with small point Cd
301 input (e.g., sub-basin outlet 1056 in Fig. 4b) indicating that nonpoint source Cd input is more
302 responsible for the exceedance.
303

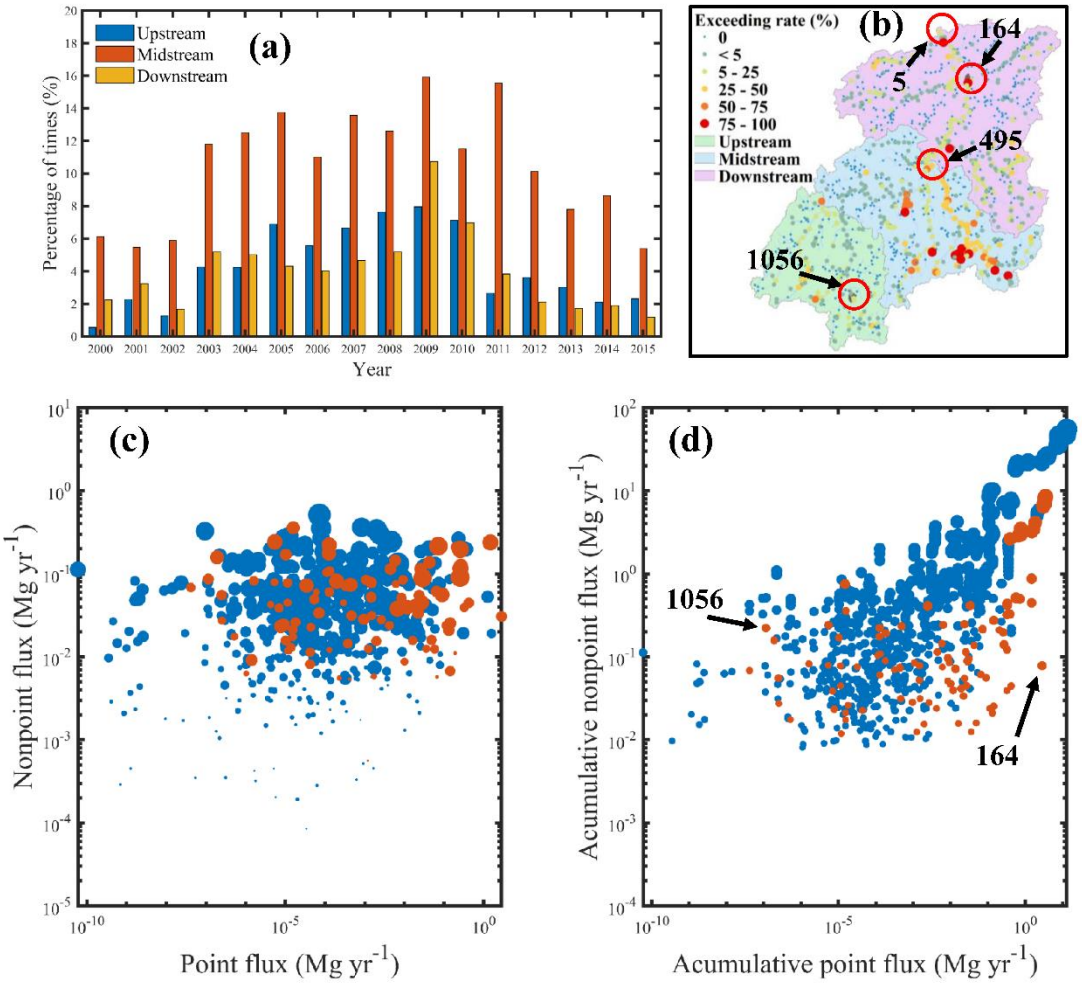

304
305 Fig. 4. (a) Percentage of times that monthly mean TCd concentrations exceeded China surface water
306 quality standard of Cd (1.0 μg L^{-1}) in the upstream, midstream, and downstream of XRB. (b)
307 Percentage of times that monthly mean TCd concentrations exceeded the water quality standard of
308 Cd (1.0 μg L^{-1}) for 1118 river sections over 16 years. (c) Comparison of point (industrial emissions)

and nonpoint source (surface runoff + lateral flow + soil erosion) Cd fluxes at the sub-basin level. Blue dots represent the non-exceeding river sections, and red dots represent the exceeding river sections. The point size indicates the sub-basin area. (d) Comparison of accumulative point and nonpoint Cd fluxes at the upstream basin level. Blue dots represent the non-exceeding river sections and red dots represent the exceeding river sections. The point size indicates the yearly mean streamflow at the sub-basin outlet. Data presented are for the period 2000 to 2015.

3.2. Changes in land-to-river Cd fluxes in different scenarios

Four management scenarios were compared with the baseline condition to evaluate their effectiveness on land-to-river fluxes in four main transport pathways: industrial emissions, surface runoff, lateral flow, and soil erosion (Fig. 5). At the basin level, both the emission reductions of the mining and smelting sectors could significantly ($p < 0.01$) reduce the industrial emissions with a range of 3.1% to 30.8% (Fig. 5a). The elimination of 50% of the smelting sector resulted in the most significant reduction (30.8%) in industrial Cd emissions, while a 50% cut in the mining sector could reduce 15.4% of industrial Cd emissions. Clearly, soil conservation and soil remediation did not affect industrial Cd emissions but significantly ($p < 0.01$) impacted other Cd pathways. Changing the soil pH had a greater influence than soil erosion control on Cd fluxes in both surface runoff and lateral flow (Fig. 5b-c). Increasing soil pH by 0.5 units could reduce surface runoff and lateral flow of Cd fluxes by 20.9% and 21.7%. Interestingly, controlling soil erosion could increase the Cd flux to the river through lateral flow (Fig. 5c). This is because infiltration and soil water increase when surface runoff decreases, leading to higher Cd fluxes through lateral flow. Soil conservation, such as terraces, has long been acknowledged as an effective way to control runoff and increase soil

moisture, leading to a greater lateral flow (Camera et al., 2012; Stanchi et al., 2012). In addition, increasing the soil pH may reduce Cd fluxes through soil erosion owing to the decreased Cd concentration in the top soil layer (Fig. 5d). Heavy metals in soil could move upward to the topsoil through evaporation-induced capillary rise (Dold and Fontboté, 2001; Lima et al., 2014). However, the decreased dissolved Cd concentration in soil pore water resulting from the pH-induced equilibrium shift limits the upward movement of Cd to the topsoil. Such effects may be caused by the declined upward migration of Cd through soil evaporation owing to the decreased Cd concentration in the soil pore water after pH increases. Additionally, the impact of climate change in this area is worth mentioning. For example, Du et al. (2013) combined the standardized precipitation index and Mann–Kendall (MK) statistical test to investigate trends of dry and wet conditions in the study area during 1951–2007. They found XRB becomes drier in spring and autumn and wetter in summer and winter. Many studies have shown that the relative contribution of different source waters varies greatly under dry and wet conditions (e.g., Li et al., 2017; Zhi et al., 2019). Such a change in climate and hydrological regime may change the mechanism of metal delivery from the upland to the river. Thus, the impacts of climate change should be evaluated to address the challenges posed by climate change on water quality improvement.

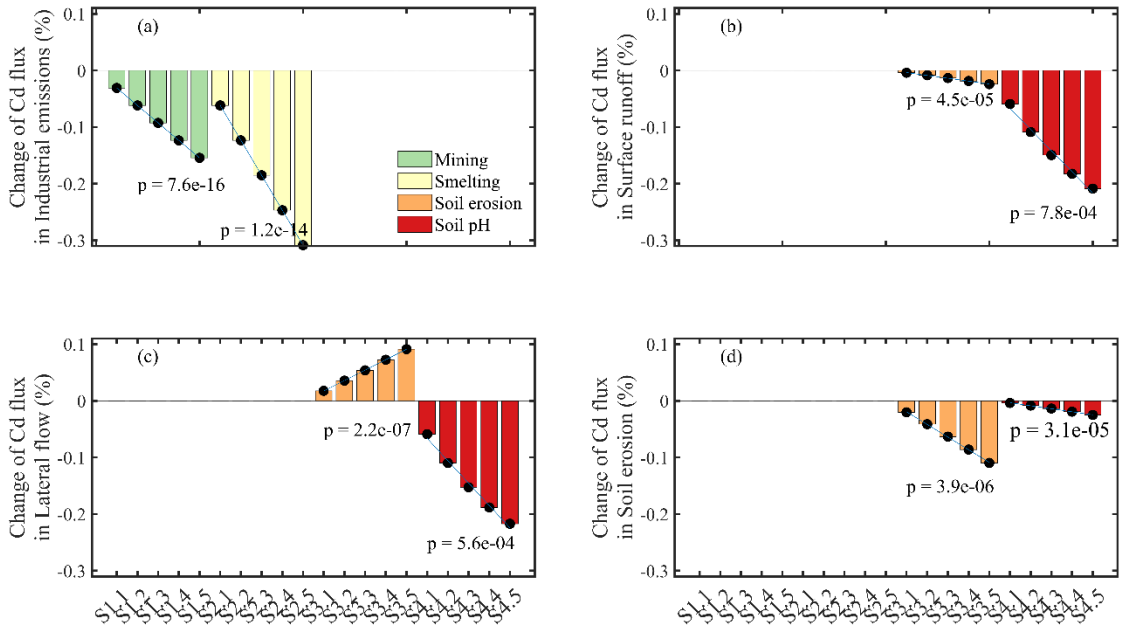

Fig. 5. Percent change of simulated land-to-river Cd fluxes (industrial emission, surface runoff, lateral flow, and soil erosion) under four management scenarios. See Table 1 for scenario descriptions.

3.3. Changes of riverine Cd loads for different scenarios

In addition to the land-to-river Cd fluxes, we investigated riverine Cd loads under four management scenarios in the XRB. The reduction in TCd loads varied across the 1186 sub-basin outlets (Fig. 6). For mining control, the sub-basin outlets with high load reduction appear mainly in the upstream and midstream reaches, especially in the Southeast Lei River (Fig. 1). In contrast, smelting control mainly reduced TCd in the midstream and downstream areas. This is reasonable because most large-scale smelting activities occur in urban areas of the XRB midstream and downstream. Soil erosion control is the only management measure that could increase the TCd load as a result of the net increase in land-to-river Cd fluxes in some sub-basins. As a practical and effective measure, changing (increasing) the soil pH resulted in a reduction in TCd, ranging from

363 53.0% to 0% across the sub-basins. Soil acidification occurs widely in Chinese croplands owing to
364 excessive nitrogen fertilization and acid precipitation (Guo et al., 2010; Zhu et al., 2018). For
365 example, a 30-year field experiment in paddy soils of XRB found that mean topsoil pH declined by
366 0.94 units from the 1980s to 2014, at a mean rate of 0.031 units yr^{-1} (Zhu et al., 2016). Acidification
367 can significantly alter the biogeochemistry of Cd in agroecosystems. A century-lasting experiment
368 at Rothamsted Experimental Station has revealed that soil acidification to pH 4 mobilized 60%–90%
369 of total soil Cd (Blake and Goulding, 2002). Therefore, agricultural land acidification should be
370 prevented to minimize Cd transport in the XRB. Liming to increase the soil pH, reducing the
371 application rate of chemical nitrogen fertilizers, and increasing organic fertilizers, such as manure,
372 could be preferentially implemented.

373 Fig. 7 shows the boxplots of the monthly DCd and PCd loads at three representative outlets
374 (outlets 1056, 495, and 5). A paired-sample t-test was used to determine whether the management
375 scenario differed from the baseline scenario (S0); the upward-pointing triangle below each boxplot
376 indicated a significant difference at the level of 0.05. Outlet 1056 (Fig. 4b) is the exceeding river
377 section with a small proportion of upstream point source input. The upstream sub-basins of outlet
378 1056 cover approximately 213 km^2 with 96 percent of them designated as nonpoint source control
379 areas (details in section 2.3). As a nonpoint-dominated site, it benefited from soil erosion control
380 (S3.1–3.5) and soil pH elevation (S4.1–4.5), as evidenced by the significant reductions of both DCd
381 and PCd (Fig. 7a-b). The outlet of sub-basin 495 (Fig. 4b) is the outlet of the Lei River, one of the
382 major tributaries in Southeast XRB. For outlet 495 (Fig. 7c-d), mining control (Scenarios 1.1–1.5)
383 led to a decline in monthly mean DCd by 5.4–28.2% and in monthly mean PCd by 5.2–25.6%. The
384 simulation results for the entire XRB outlet (Outlet 5 in Fig. 4b) indicated that maximal

385 improvements were achieved when implementing emission control of smelting sectors (Scenarios
386 2.1–2.5 in Fig. 7e-f). For example, scenario 2.5 could significantly ($p < 0.05$) decrease the monthly
387 mean loads of DCd from 940 to 720 kg and of PCd from 2,150 to 1,760 kg. It should be noted that
388 soil conservation scenarios did not reduce the DCd and PCd at the entire XRB outlet (Fig. 7e-f).

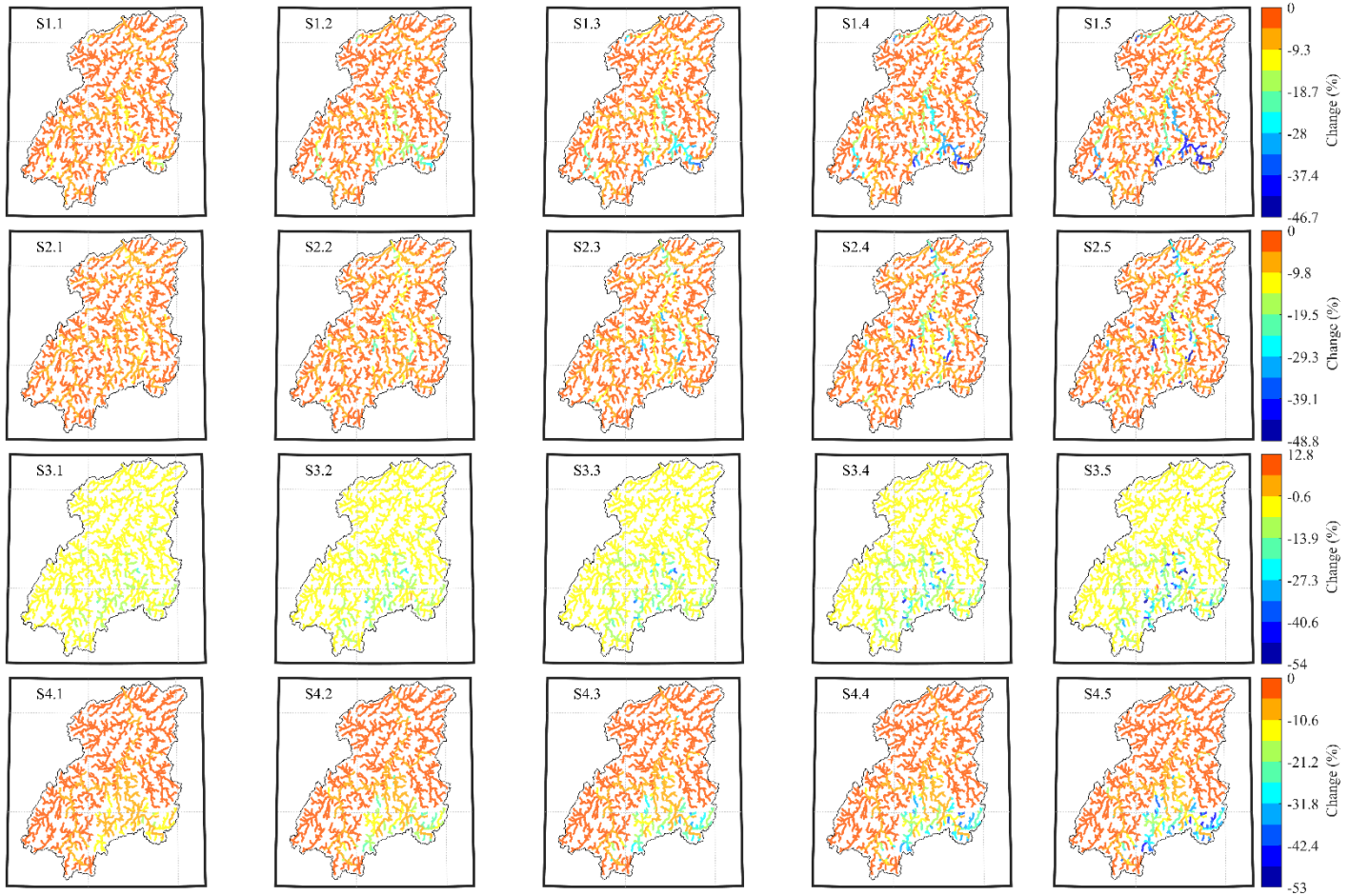

389

390 Fig. 6. Percent change (%) of simulated TCd loads over 2000–2015 across the 1118 sub-basin outlets under four management scenarios. See Table 1 for scenario

391 descriptions.

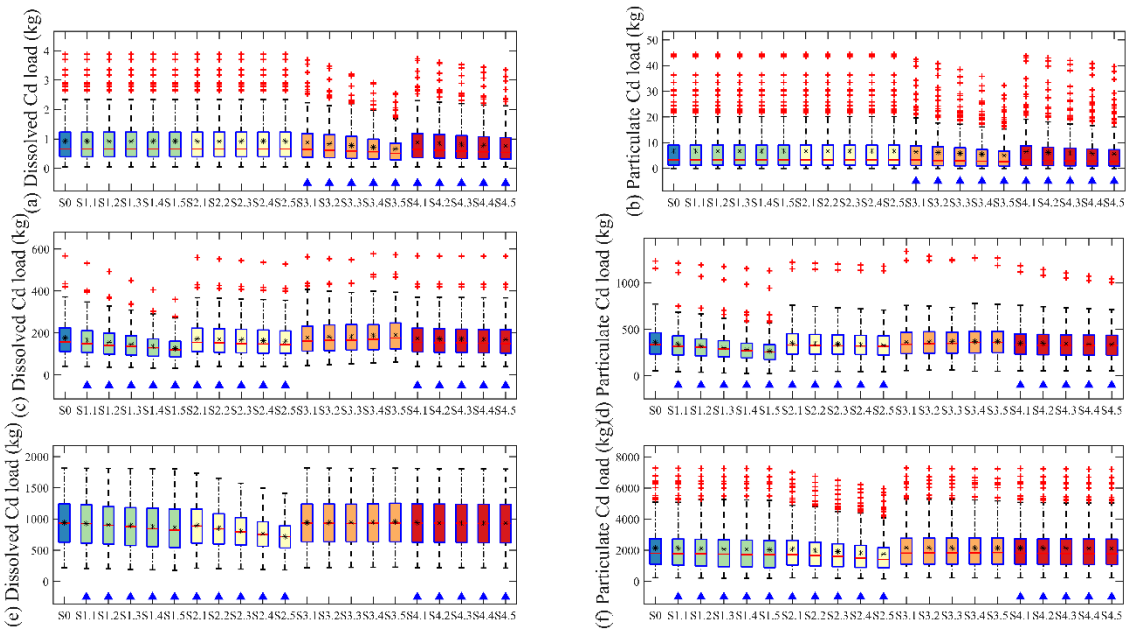

Fig. 7. Boxplots of simulated monthly DCd and PCd loads at outlets 1056 (a, b), 495 (c, d), and 5 (e, f) under four management scenarios. Each boxplot represents 192 monthly Cd loads from 2000–2015 for each scenario. Outliers are classified as all points outside 1.5 times the interquartile range above the upper quartile and below the lower quartile, and the outliers are plotted individually using the '+' marker symbol. Black asterisk points represent mean values. The upward-pointing triangle below each boxplot indicated a significant difference between management scenario and baseline scenario at the significance level of 0.05. See Table 1 for scenario descriptions.

3.4. Watershed-scale Cd budgets reveal the effectiveness of management measures

Owing to the unexpected results of the limited reduction of riverine Cd loads under soil conservation scenarios, we further examined the complete watershed-average Cd fluxes in both land and in-stream phases. As shown in Fig. 8a, the implementation of soil erosion control (S3.1–3.5) decreased the PCd flux (−5,328 to −981 kg yr^{-1}) in soil erosion and slightly increased the DCd fluxes (15–65 kg yr^{-1}) through surface and subsurface flow. Overall, this resulted in a reduction in the total

Cd fluxes to the river. However, the riverine TCd load at the XRB outlet did not decrease as expected but increased slightly. This is because the net retention (settling−resuspension) of Cd in the stream also decreased. Moreover, the reduction in Cd retention was greater than that in the land-to-river Cd load. Therefore, a quantitative understanding of the variable importance of point and nonpoint sources of pollution, as well as the instream processes of metal attenuation and release, is crucial for evaluating the effects of measures on downstream water quality. It should be noted that although soil conservation measures do not benefit the riverine Cd load, they can curb the accumulation of Cd in river sediments. For example, the time series of yearly mean Cd concentration in the sediment of 196 polluted river sections showed that soil erosion control could reduce the Cd accumulation in sediment at the end of 2015 by 0.1–15.2% under S3.1–S3.5 (Fig. 8b). A frequent occurrence of heavy floods was witnessed across the XRB (Du et al., 2019), which may flush these sediment-bound metals downstream during high-flow events. Recent studies have analyzed the simulated climate extreme indices from 18 CMIP6 models and found that all regions of China witnessed an increase in extreme precipitation (Zhu et al., 2021). For example, the areal-mean 95th percentile precipitation would increase remarkably by 16.5%, 25.4%, and 46.5% for the 1.5, 2, and 3 °C global warming levels, respectively, with respect to the reference period of 1985–2005. Therefore, modified or new strategies may be required to minimize the potential negative impacts of climate change, for example, on river sediment dynamics, to meet future water quality targets.

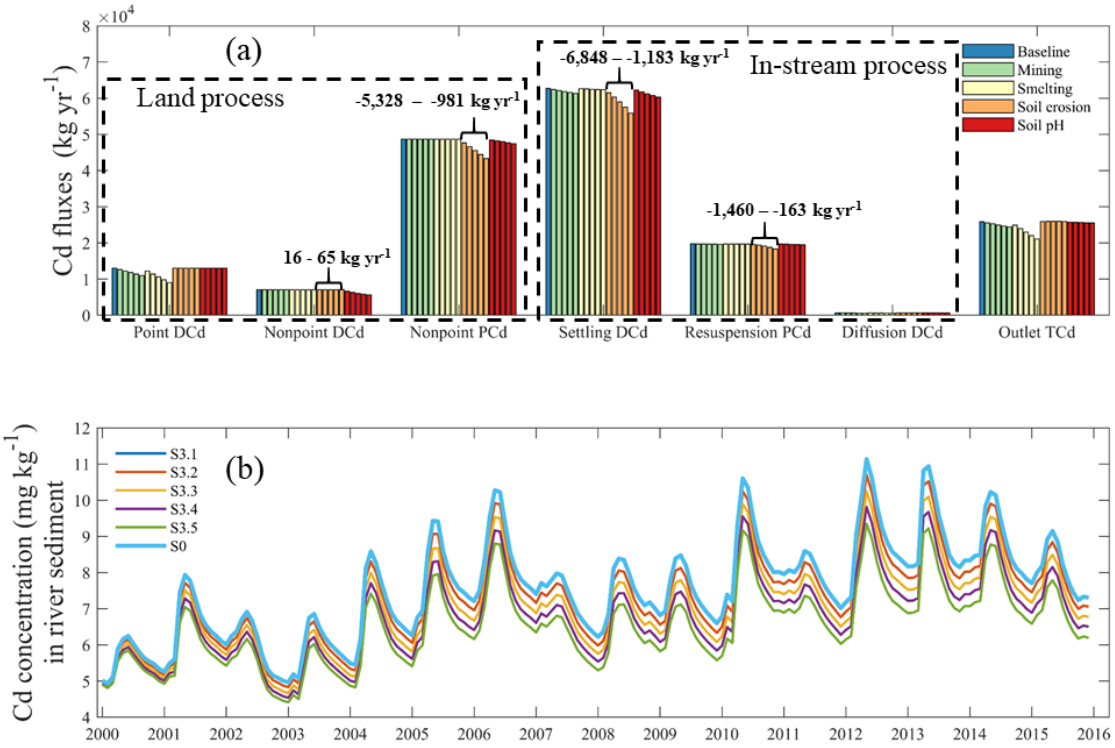

Fig. 8. (a) Simulated Cd fluxes (kg yr^{-1}) in land and in-stream phases of XRB. (b) The time series (2000–2015) of monthly mean Cd concentrations (mg kg^{-1}) in the sediment of river sections where river water TCd concentrations exceeded water quality standard of 1 μg L^{-1}. See Table 1 for scenario descriptions.

4. Conclusions

In this study, we applied a process-based watershed-scale Cd model within a scenario analysis framework to understand and evaluate the effects of different management practices on land-to-river Cd fluxes and riverine Cd loads in an industrialized river basin with both point and nonpoint source pollution. Based on our findings, we recommend several key management measures for achieving water quality targets in river basins with Cd pollution.

(1) Effective remediation requires a comprehensive understanding of the relative contributions of metals from all important sources in a basin, and that understanding must be based on spatially detailed quantification of metal loads in different pathways. In addition, both loads from the upstream channels and the corresponding sub-basin should be considered. Furthermore, it is important to consider the dynamics of metals in the river network because in-stream processes may significantly affect the riverine metal load at the downstream outlets. Numerical models such as the SWAT-HM can be valuable tools to simulate metal fate and transport in both land and river phases to develop remediation strategies.

(2) Different management measures will yield diverse outcomes. For example, reducing the riverine Cd load at the XRB outlet could be achieved by cutting the point source Cd emissions from the smelting sector rather than the mining sector, owing to their different spatial distributions. Controlling soil erosion may decrease the PCd flux into rivers while increasing the DCd flux, thereby affecting the riverine Cd load to a limited extent. However, controlling soil erosion could be an effective way to restrain heavy metal accumulation in river sediments. In addition, increasing the soil pH could be a practical and effective measure for reducing the nonpoint Cd loads in nonpoint-dominated sub-basins.

(3) Targeted remedial strategies should be implemented for water quality management of large river basins, such as the XRB. For example, a zoning control scheme can be proposed that includes point source control areas, nonpoint source control areas, and mixed-source control areas. Given that smelting and mining are the two major drivers of water quality deterioration in most parts of the XRB, industrial emission reductions need to be maintained. In addition, soil remediation could be implemented by increasing soil pH in nonpoint and mixed-source control areas. Moreover, incorporating climate change considerations and assessing the proposed management scenarios for their climate vulnerabilities will build more resilience in confronting future conditions.

Notes

The authors declare no competing financial interest.

Data availability

The data will be made available upon reasonable request. The SWAT-HM model is available at https://github.com/LyntonZhou/SWAT-HM-pre-post-processing.

Acknowledgements

This work was supported by the National Natural Science Foundation of China (42107425), the National Key Research and Development Program (2021YFC3201000, 2021YFC3201001), and the

China Postdoctoral Science Foundation (2021M702959). The authors thank Dr. Chunming Sui from ETH Zurich for the fruitful discussions.

References

Abbaspour, K.C. (2015) SWAT-CUP: SWAT calibration and uncertainty programs—a user manual. Eawag: Dübendorf, Switzerland, 16-70.

Aoshima, K. (2016) Itai-itai disease: Renal tubular osteomalacia induced by environmental exposure to cadmium—historical review and perspectives. Soil Science and Plant Nutrition 62(4), 319-326. https://doi.org/10.1080/00380768.2016.1159116.

Arabi, M., Frankenberger, J.R., Engel, B.A. and Arnold, J.G. (2007) Representation of agricultural conservation practices with SWAT. Hydrological Processes 22(16), 3042-3055. https://doi.org/10.1002/hyp.6890.

Arnold, J.G., Srinivasan, R., Muttiah, R.S. and Williams, J.R. (1998) Large area hydrologic modeling and assessment part I: Model development. JAWRA Journal of the American Water Resources Association 34(1), 73-89. https://doi.org/10.1111/j.1752-1688.1998.tb05961.x.

Blake, L. and Goulding, K.W.T. (2002) Effects of atmospheric deposition, soil pH and acidification on heavy metal contents in soils and vegetation of semi-natural ecosystems at Rothamsted Experimental Station, UK. Plant and Soil 240(2), 235-251. https://doi.org/10.1023/A:1015731530498.

Byrne, P., Onnis, P., Runkel, R.L., Frau, I., Lynch, S.F.L. and Edwards, P. (2020) Critical shifts in trace metal transport and remediation performance under future low river flows. Environmental Science & Technology 54(24), 15742-15750. https://doi.org/10.1021/acs.est.0c04016.

Camera, C., Masetti, M. and Apuani, T. (2012) Rainfall, infiltration, and groundwater flow in a terraced slope of Valtellina (Northern Italy): field data and modelling. Environmental Earth Sciences 65(4), 1191-1202. https://doi.org/10.1007/s12665-011-1367-3.

Chen, H., Zhang, W., Yang, X., Wang, P., McGrath, S.P. and Zhao, F.-J. (2018) Effective methods to reduce cadmium accumulation in rice grain. Chemosphere 207, 699-707. https://doi.org/10.1016/j.chemosphere.2018.05.143.

Degryse, F., Smolders, E. and Parker, D.R. (2009) Partitioning of metals (Cd, Co, Cu, Ni, Pb, Zn) in soils: concepts, methodologies, prediction and applications – a review. European Journal of Soil Science 60(4), 590-612. https://doi.org/10.1111/j.1365-2389.2009.01142.x.

Dold, B. and Fontboté, L. (2001) Element cycling and secondary mineralogy in porphyry copper tailings as a function of climate, primary mineralogy, and mineral processing. Journal of Geochemical Exploration 74(1), 3-55. https://doi.org/10.1016/S0375-6742(01)00174-1.

Du, J., Cheng, L. and Zhang, Q. (2019) Spatiotemporal variability and trends in the hydrology of the Xiang River basin, China: extreme precipitation and streamflow. Arabian Journal of Geosciences 12(18), 566. https://doi.org/10.1007/s12517-019-4731-3.

Du, J., Fang, J., Xu, W. and Shi, P. (2013) Analysis of dry/wet conditions using the standardized precipitation index and its potential usefulness for drought/flood monitoring in Hunan Province, China. Stochastic Environmental Research and Risk Assessment 27(2), 377-387. https://doi.org/10.1007/s00477-012-0589-6.

514 Guo, J.H., Liu, X.J., Zhang, Y., Shen, J.L., Han, W.X., Zhang, W.F., Christie, P., Goulding, K.W.T.,
515 Vitousek, P.M. and Zhang, F.S. (2010) Significant Acidification in Major Chinese Croplands.
516 Science 327(5968), 1008-1010. https://doi.org/10.1126/science.1182570.
517 Han, C., Qin, Y., Zheng, B., Ma, Y., Zhang, L. and Cao, W. (2014) Sediment quality assessment for heavy
518 metal pollution in the Xiang-jiang River (China) with the equilibrium partitioning approach.
519 Environmental Earth Sciences 72(12), 5007-5018. https://doi.org/10.1007/s12665-014-3368-5.
520 Holland, J.E., Bennett, A.E., Newton, A.C., White, P.J., McKenzie, B.M., George, T.S., Pakeman, R.J.,
521 Bailey, J.S., Fornara, D.A. and Hayes, R.C. (2018) Liming impacts on soils, crops and
522 biodiversity in the UK: A review. Science of The Total Environment 610-611, 316-332.
523 https://doi.org/10.1016/j.scitotenv.2017.08.020.
524 Hou, D. and Li, F. (2017) Complexities Surrounding China's Soil Action Plan. Land Degradation &
525 Development 28(7), 2315-2320. https://doi.org/10.1002/ldr.2741.
526 Hu, H., Jin, Q. and Kavan, P. (2014) A Study of Heavy Metal Pollution in China: Current Status,
527 Pollution-Control Policies and Countermeasures. Sustainability 6(9), 5820-5838.
528 https://doi.org/10.3390/su6095820.
529 Hu, Y., Cheng, H. and Tao, S. (2016) The Challenges and Solutions for Cadmium-contaminated Rice in
530 China: A Critical Review. Environment International 92-93, 515-532.
531 https://doi.org/10.1016/j.envint.2016.04.042.
532 Hunt, N.D., Hill, J.D. and Liebman, M. (2019) Cropping System Diversity Effects on Nutrient Discharge,
533 Soil Erosion, and Agronomic Performance. Environmental Science & Technology 53(3), 1344-
534 1352. https://doi.org/10.1021/acs.est.8b02193.
535 IARC (2018) IARC monographs on the evaluation of carcinogenic risks to humans.
536 Jarvis, A.P., Davis, J.E., Orme, P.H.A., Potter, H.A.B. and Gandy, C.J. (2019) Predicting the Benefits of
537 Mine Water Treatment under Varying Hydrological Conditions using a Synoptic Mass Balance
538 Approach. Environmental Science & Technology 53(2), 702-709.
539 https://doi.org/10.1021/acs.est.8b06047.
540 Jiao, W., Ouyang, W., Hao, F., Huang, H., Shan, Y. and Geng, X. (2014) Combine the soil water
541 assessment tool (SWAT) with sediment geochemistry to evaluate diffuse heavy metal loadings
542 at watershed scale. Journal of Hazardous Materials 280, 252-259.
543 https://doi.org/10.1016/j.jhazmat.2014.07.081.
544 Kast, J.B., Kalcic, M., Wilson, R., Jackson-Smith, D., Breyfogle, N. and Martin, J. (2021) Evaluating the
545 efficacy of targeting options for conservation practice adoption on watershed-scale phosphorus
546 reductions. Water Research 201, 117375. https://doi.org/10.1016/j.watres.2021.117375.
547 Kicińska, A., Pomykała, R. and Izquierdo-Diaz, M. (2022) Changes in soil pH and mobility of heavy
548 metals in contaminated soils. European Journal of Soil Science 73(1), e13203.
549 https://doi.org/10.1111/ejss.13203.
550 Kubier, A., Wilkin, R.T. and Pichler, T. (2019) Cadmium in soils and groundwater: A review. Applied
551 Geochemistry 108, 104388. https://doi.org/10.1016/j.apgeochem.2019.104388.
552 Kumar, V., Parihar, R.D., Sharma, A., Bakshi, P., Singh Sidhu, G.P., Bali, A.S., Karaouzas, I., Bhardwaj,
553 R., Thukral, A.K., Gyasi-Agyei, Y. and Rodrigo-Comino, J. (2019) Global evaluation of heavy
554 metal content in surface water bodies: A meta-analysis using heavy metal pollution indices and
555 multivariate statistical analyses. Chemosphere 236, 124364.
556 https://doi.org/10.1016/j.chemosphere.2019.124364.
557 Lei, M., Tie, B.-q., Song, Z.-g., Liao, B.-H., Lepo, J.E. and Huang, Y.-z. (2015) Heavy metal pollution

and potential health risk assessment of white rice around mine areas in Hunan Province, China. Food Security 7(1), 45-54. https://doi.org/10.1007/s12571-014-0414-9.

Li, L., Bao, C., Sullivan, P.L., Brantley, S., Shi, Y. and Duffy, C. (2017) Understanding watershed hydrogeochemistry: 2. Synchronized hydrological and geochemical processes drive stream chemostatic behavior. Water Resources Research 53(3), 2346-2367. https://doi.org/10.1002/2016WR018935.

Li, X., Zhao, Z., Yuan, Y., Wang, X. and Li, X. (2018) Heavy metal accumulation and its spatial distribution in agricultural soils: evidence from Hunan province, China. RSC Advances 8(19), 10665-10672. https://doi.org/10.1039/C7RA12435J.

Lima, A.T., Safar, Z. and Loch, J.P.G. (2014) Evaporation as the transport mechanism of metals in arid regions. Chemosphere 111, 638-647. https://doi.org/10.1016/j.chemosphere.2014.05.027.

Liu, M., Zhang, Q., Ge, S., Mason, R.P., Luo, Y., He, Y., Xie, H., Sa, R., Chen, L. and Wang, X. (2019) Rapid increase in the lateral transport of trace elements induced by soil erosion in major karst regions in China. Environmental Science & Technology 53(8), 4206-4214. https://doi.org/10.1021/acs.est.8b06143.

Meng, Y., Zhou, L., He, S., Lu, C., Wu, G., Ye, W. and Ji, P. (2018) A heavy metal module coupled with the SWAT model and its preliminary application in a mine-impacted watershed in China. Science of The Total Environment 613-614, 1207-1219. https://doi.org/10.1016/j.scitotenv.2017.09.179.

MEPPRC and MLRPRC (2014) Reports on China's Soil Pollution Survey, Chinese Environment Science Press, Beijing.

Motovilov, Y.G. and Fashchevskaya, T.B. (2019) Simulation of spatially-distributed copper pollution in a large river basin using the ECOMAG-HM model. Hydrological Sciences Journal 64(6), 739-756. https://doi.org/10.1080/02626667.2019.1596273.

Nair, S.S., DeRolph, C., Peterson, M.J., McManamay, R.A. and Mathews, T. (2022) Integrated watershed process model for evaluating mercury sources, transport, and future remediation scenarios in an industrially contaminated site. Journal of Hazardous Materials 423, 127049. https://doi.org/10.1016/j.jhazmat.2021.127049.

Nziguheba, G. and Smolders, E. (2008) Inputs of trace elements in agricultural soils via phosphate fertilizers in European countries. Science of The Total Environment 390(1), 53-57. https://doi.org/10.1016/j.scitotenv.2007.09.031.

Qin, Y., Han, C., Zhang, L., Zheng, B. and Cao, W. (2012) Distribution of heavy metals among surface water,suspended solids and surface sediments in Hengyang section of Xiangjiang River. Acta entiae Circumstantiae 32(11), 2836-2844.

Satarug, S., Baker, J.R., Urbenjapol, S., Haswell-Elkins, M., Reilly, P.E.B., Williams, D.J. and Moore, M.R. (2003) A global perspective on cadmium pollution and toxicity in non-occupationally exposed population. Toxicology Letters 137(1), 65-83. https://doi.org/10.1016/S0378-4274(02)00381-8.

Satarug, S., Vesey, D.A. and Gobe, G.C. (2017) Current health risk assessment practice for dietary cadmium: Data from different countries. Food and Chemical Toxicology 106, 430-445. https://doi.org/10.1016/j.fct.2017.06.013.

Shen, Z., Zhong, Y., Huang, Q. and Chen, L. (2015) Identifying non-point source priority management areas in watersheds with multiple functional zones. Water Research 68, 563-571. https://doi.org/10.1016/j.watres.2014.10.034.

Shi, J.-J., Shi, Y., Feng, Y.-L., Li, Q., Chen, W.-Q., Zhang, W.-J. and Li, H.-Q. (2019) Anthropogenic cadmium cycles and emissions in Mainland China 1990–2015. Journal of Cleaner Production 230, 1256-1265. https://doi.org/10.1016/j.jclepro.2019.05.166.

Smolders, E. and Mertens, J. (2013) Heavy metals in soils: Trace metals and metalloids in soils and their bioavailability. Alloway, B.J. (ed), pp. 283-311, Springer Netherlands, Dordrecht.

Stanchi, S., Freppaz, M., Agnelli, A., Reinsch, T. and Zanini, E. (2012) Properties, best management practices and conservation of terraced soils in Southern Europe (from Mediterranean areas to the Alps): A review. Quaternary International 265, 90-100. https://doi.org/10.1016/j.quaint.2011.09.015.

Sui, C., Fatichi, S., Burlando, P., Weber, E. and Battista, G. (2022) Modeling distributed metal pollution transport in a mine impacted catchment: Short and long-term effects. Science of The Total Environment 812, 151473. https://doi.org/10.1016/j.scitotenv.2021.151473.

Tuppad, P., Kannan, N., Srinivasan, R., Rossi, C.G. and Arnold, J.G. (2010) Simulation of Agricultural Management Alternatives for Watershed Protection. Water Resources Management 24(12), 3115-3144. https://doi.org/10.1007/s11269-010-9598-8.

Ulrich, A.E. (2019) Cadmium governance in Europe's phosphate fertilizers: Not so fast? Science of The Total Environment 650, 541-545. https://doi.org/10.1016/j.scitotenv.2018.09.014.

Velleux, M.L., England, J.F. and Julien, P.Y. (2008) TREX: Spatially distributed model to assess watershed contaminant transport and fate. Science of The Total Environment 404(1), 113-128. https://doi.org/10.1016/j.scitotenv.2008.05.053.

Whitehead, P.G., Butterfield, D. and Wade, A.J. (2009) Simulating metals and mine discharges in river basins using a new integrated catchment model for metals: pollution impacts and restoration strategies in the Aries-Mures river system in Transylvania, Romania. Hydrology Research 40(2-3), 323-346. https://doi.org/10.2166/nh.2009.069.

WHO (2010) Exposure to cadmium: a major public health concern, pp. 3-6.

Williams, P.N., Lei, M., Sun, G., Huang, Q., Lu, Y., Deacon, C., Meharg, A.A. and Zhu, Y.-G. (2009) Occurrence and Partitioning of Cadmium, Arsenic and Lead in Mine Impacted Paddy Rice: Hunan, China. Environmental Science & Technology 43(3), 637-642. https://doi.org/10.1021/es802412r.

Xie, H., Chen, L. and Shen, Z. (2015) Assessment of Agricultural Best Management Practices Using Models: Current Issues and Future Perspectives. Water 7(3), 1088-1108. https://doi.org/10.3390/w7031088.

Zhang, Q., Li, Z., Zeng, G., Li, J., Fang, Y., Yuan, Q., Wang, Y. and Ye, F. (2008) Assessment of surface water quality using multivariate statistical techniques in red soil hilly region: a case study of Xiangjiang watershed, China. Environmental Monitoring and Assessment 152(1), 123. https://doi.org/10.1007/s10661-008-0301-y.

Zhi, W., Li, L., Dong, W., Brown, W., Kaye, J., Steefel, C. and Williams, K.H. (2019) Distinct Source Water Chemistry Shapes Contrasting Concentration-Discharge Patterns. Water Resources Research 55(5), 4233-4251. https://doi.org/10.1029/2018WR024257.

Zhou, L., Meng, Y., Vaghefi, S.A., Marras, P.A., Sui, C., Lu, C. and Abbaspour, K.C. (2020) Uncertainty-based metal budget assessment at the watershed scale: Implications for environmental management practices. Journal of Hydrology 584, 124699. https://doi.org/10.1016/j.jhydrol.2020.124699.

Zhou, L., Teng, M., Song, F., Zhao, X., Wu, F., Huang, Y. and Abbaspour, K.C. (2023) Modeling land-

to-river Cd fluxes and riverine Cd loads to inform management decisions. Journal of Environmental Management 334, 117501. https://doi.org/10.1016/j.jenvman.2023.117501.

Zhou, Y., Wang, L., Xiao, T., Chen, Y., Beiyuan, J., She, J., Zhou, Y., Yin, M., Liu, J., Liu, Y., Wang, Y. and Wang, J. (2020) Legacy of multiple heavy metal(loid)s contamination and ecological risks in farmland soils from a historical artisanal zinc smelting area. Science of The Total Environment 720, 137541. https://doi.org/10.1016/j.scitotenv.2020.137541.

Zhu, H., Chen, C., Xu, C., Zhu, Q. and Huang, D. (2016) Effects of soil acidification and liming on the phytoavailability of cadmium in paddy soils of central subtropical China. Environmental Pollution 219, 99-106. https://doi.org/10.1016/j.envpol.2016.10.043.

Zhu, H., Jiang, Z. and Li, L. (2021) Projection of climate extremes in China, an incremental exercise from CMIP5 to CMIP6. Science Bulletin 66(24), 2528-2537. https://doi.org/10.1016/j.scib.2021.07.026.

Zhu, Q., de Vries, W., Liu, X., Hao, T., Zeng, M., Shen, J. and Zhang, F. (2018) Enhanced acidification in Chinese croplands as derived from element budgets in the period 1980–2010. Science of The Total Environment 618, 1497-1505. https://doi.org/10.1016/j.scitotenv.2017.09.289.

Zhuang, Y., Zhang, L., Du, Y. and Chen, G. (2016) Current patterns and future perspectives of best management practices research: A bibliometric analysis. Journal of Soil and Water Conservation 71(4), 98A. https://doi.org/10.2489/jswc.71.4.98A.